Proc. Eurohaptics, August 2002, Edinburgh, Scotland, pp. 110-115

Haptic Rendering of Tool Contact

Mohsen Mahvash[1], Vincent Hayward[2] and John Lloyd[3]

[1,2]Center For Intelligent Machines
McGill University, Montréal, Québec, H3A 2A7 Canada
mahvash|hayward@cim.mcgill.ca

[3]Department of Computer Science
University of British Colombia, V6T 1Z4 Canada
lloyd@cs.ubc.ca

Abstract

Virtual haptic interaction with simulated deformable bodies requires contact forces to be computed with reasonable approximations in real time. This paper makes use of St. Venant's principle on concentrated loads, and Castigliano's theory on deflection to show that when an elastic body is globally deformed, the point-force representation of a tool contact is a good approximation. However, when the deformation of the body is localized in a small region, the contact forces critically depend on the shape of the tool. Previously proposed approaches based on finite element and boundary element methods to predict deformation can not always be used to simulate tool contact. We propose a model for computing tool force-displacement responses which is efficiently calculated at run time by interpolation of pre-calculated force-deflection responses, each representing the response of a contact between a given tool and a body. The interpolation approach ensures the continuity of the rendered force, although this force is obtained from pre-calculated responses at a set of discrete surface points. The paper also describes how sliding contacts can be modeled by computing tangential friction forces in terms of pre-sliding displacements over the surface of the undeformed body. Tests involving two deformation types and various contact forms were performed on samples of rubber and of calf liver. A computer implementation is also described.

1 Introduction

During haptic rendering, the forces resulting from a point contact with a rigid body are used to represent the shape, texture, and the position of a body [17, 15]. When this body is deformable, the contact forces must simulate the details of the interaction because these forces depend on the elastic properties of the body, on how the body is supported, and most critically, on the tool used. An accurate representation of these factors has importance for surgical simulators and other applications.

The point contact representation used for rendering rigid bodies is not always sufficient. When an elastic body is globally deformed, a point representation can suffice to predict the contact forces, but when the deformation of the body is localized around the contact point, the contact forces critically depend on the shape of the tool that deforms the body. The consideration of small tool tips and small contact areas does not eliminate the dependency of the interaction on tool shape, quite the opposite is true. The force response of a contact interaction with localized deformation essentially depends on two inputs: the contact area and the distribution of deflection over that area.

A contact that causes local deformation cannot be properly simulated by present approaches [1, 3, 5, 18, 4, 8, 16, 2]. In all these approaches, the tool force must be computed from forces acting at vertices located in a contact region determined by interference detection. The point contact region may contain only one vertex, or a few vertices, according to arbitrary factors such as element size and shape. The number of vertices must remain limited due to the real time constraint on computations of large scale models. The deflection at the interaction point then results in a force that also depends on the element size and shape, when in fact the force of a contact interaction with localized deformation should depend only on deflection and on the area of deflection. In [9], a point contact was modeled by a predetermined distribution of traction over a fixed contact area, but the change of the contact area and the distribution of traction due to shape and movement of the tool was not con-

sidered.

This paper introduces a model for haptic rendering of contact of a tool with an elastic body which causes localized deformation. The tool shape is presently restricted to axis symmetrical shapes, but any tool could in principle be programmed. Interaction forces are evaluated at run time by interpolation of pre-calculated force-deflection responses, each representing the response to the mechanical interaction between a given tool and a body. The storage requirement are actually quite modest.

Please note that nowhere in this paper, the assumptions of material homogeneity, isotropy, and linear elasticity are required. It is also likely that the consideration of contacts that involve localized deformation covers a great number of cases encountered in surgical simulation problems. This is the case, for example, of all simulations which simulate palpation with a tool that does not cause damage to the tissues.

Section 2, examines the effect of tool shape. Section 3, presents a model for haptic rendering with localized deformation. Tests are described in Section 4 and the results discussed. An implementation is presented in Section 5 before concluding.

2 Effect of Tool Shape

Consider different tool shapes acting separately at the same point of a firmly held elastic body, such that the contact area always belongs to S, a small area at the point of contact which is invariant for all interactions at this point, see Figure 1. St. Venant's principle states that:

> "If the forces acting on a small area of a body are replaced by a statically equivalent system of forces acting on the same area, there will be considerable changes in local stress distribution, but the effect at distances large compared with the area on which the forces act will be negligible".

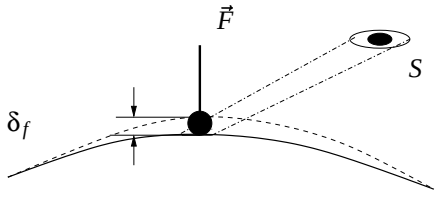

Figure 1: An interaction between a linear elastic body and a tool shape in which contact area always belongs to S.

Applying this to all possible interactions over S with a single acting force F, the stress distribution, and consequently the stored elastic energy far away from the contact place, is almost independent of the distribution of traction over S, and accordingly, to the tool shape of each interaction. Therefore for interactions over S with global deformation in which elastic energy is distributed over entire body, the total elastic energy of the body depends on the tool force alone.

Castigliano's theory's on deflection applied to interactions at S which cause global deformation together with almost uniform displacement over S, predicts the deflection of each point of S in the direction of the tool force F to be:

$$\delta_f = \frac{\partial U(F)}{\partial F}, \tag{1}$$

where U is the elastic energy of the interaction. Please see [11] for the proof of theory and for the precise definition of δ_f according to the components of the deflection of each points of contact inside the surface S. Equation (1) is almost independent of tool shape, therefore a point representation for tool contact is sufficient. Figure 2a shows an example of interaction with global deformation.

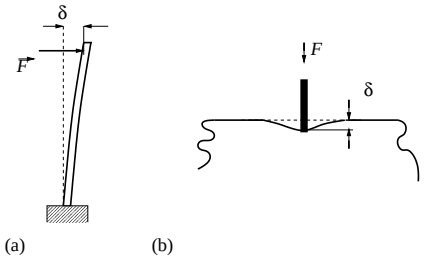

Figure 2: (a) An interaction with global deformation (b) An interaction with localized deformation.

To see that tool shape has a significant effect on the interaction force with localized deformation, it is sufficient to consider the force-deflection response to a normal contact of a small cylindrical tool shape with an infinite half space [10] (Figure 2b):

$$F = 2RE^*\delta, \tag{2}$$

where R is the radius of the tool tip and E^* is defined in terms of the Young's modulus, and Poisson's ratio of the material (see Table 1). The response for each tool depends on its radius.

In Section 4, experiments are described which confirm the predicted tool effects.

3 Model for Localized Deformation

Here, the tool is assumed to have axis symmetrical shape, however, the modeling procedure is independent of any particular shape. We consider the case of a smooth body

surface that is meshed into triangular elements, but we insist on the fact that the approach is completely independent from any particular geometrical representation of the body.

The tip of the tool is linked to the movements of the haptic device. When the tool interferes with the body, the projection of the tool tip over the undeformed body surface defines a point. The distance between this point and the tool tip defines the deflection. This definition of a contact point is in actually similar to the definition of a "god-object" in the rendering of rigid bodies [17].

For interactions at all points inside an element, the normal force, F_n, is evaluated by interpolation of three pre-calculated force-deflection responses, each representing the response to the mechanical interaction a given tool at each vertex:

$$F_n = \sum_{i=j,k,l} n_i^e(X)\, f_i(\delta) U_i \tag{3}$$

where X is a contact point, δ is the deflection at that point and for vertex i: n_i^e is the interpolation function of element e, f_i is the pre-calculated force-deflection response of a normal contact, and U_i is the unit normal vector. n_i^e for $i = j$ may be selected to be:

$$n_j^e(X) = \frac{A_{k-l}(X)}{A^e} \tag{4}$$

where A^e is the area of the element e and A_{k-l} is the area of the triangle formed by the contact point X and the nodes k and l, see Figure 3. Interpolation functions such as n_i^e based on natural coordinates are typically used in finite element and boundary element methods to ensure continuity over the surface of the body [14].

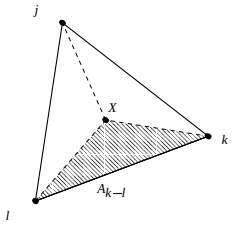

Figure 3: Area coordinates for a triangular element.

In a preprocessing step, the responses are prepared and stored. This step can be carried out offline with standard finite element code or via measurements made on samples. The storage requirements are actually small. Suppose that each function and its corresponding normal vector is represented by 20 parameters, and that each parameters in turn is represented by a single precision floating point number. To represent the nonlinear response of the entire human body (2 m^2) at a 1 mm resolution, 2 million vertices would be needed. The required 160 Mbyte of memory can easily be provided by most commodity computer!

Geometry	Normal Force
Flat R	$2RE^*\delta$
Sphere R	$\frac{4}{3}\sqrt{R}E^*\delta^{3/2}$
Cone α	$\frac{2}{\pi}tan(\alpha)E^*\delta^2$

Table 1: Force-deflection responses for axis-symmetrical contact of tool shapes with an infinite elastic body. $E^* = \frac{E}{1-\nu^2}$ where E is Young's modulus and ν Poisson's ratio of the material (results from [10]).

To represent sliding contacts, tangential forces arising from friction are modeled empirically in terms of pre-sliding displacements over the surface of the undeformed body using the method of [7] (Section 3.1). The friction forces at the sliding limit are μf_n where μ is the limiting friction coefficient and f_n is the amplitude of the normal force. It is possible to ignore the effect of the sliding contact over the normal force. This is similar to the approximation used in contact mechanics [10]. In Section 4, a test made with a piece of rubber and a steel tool shows that this approximation is actually quite good.

Analytical solutions to normal contact of axis-symmetrical tools with an infinite elastic body are reasonable approximation to force-deflection responses of interactions with significantly localized deformation over a large smooth body. Table 1 lists the force-deflection responses for a variety of theses tool shapes.

4 Tests

Tests were performed to assess the effect of tool shape during interaction with local and global deformation, as well as the effect of friction forces on normal force during a sliding contact.

A robot manipulator created programmed deflections on samples and a force sensor measured the force response for different tools, see Figure 4a. During all tests, the robot moved the tool at 1 mm/s. The samples were bonded to a metallic plate. The tool shapes were two spherical ends of 3.2 mm and 12.7 mm in diameter, and one flat end of 3.2 mm, see Figure 4b. These were carried out with ACME, the Active Measurement Facility developed at the University of British Columbia [13].

4.1 Case of Global Deformation

In the first test, we investigated the effect of tool shape on the force-deflection response of interactions that caused

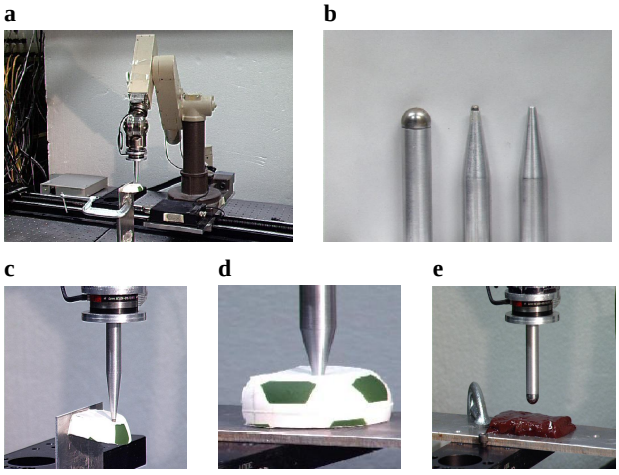

Figure 4: **a)** ACME's manipulator performing a contact test, **b)** Overview of tools, **c)** Contact with global deformation, **d)** Normal contact with local deformation, **e)** Normal contact with a fresh piece of liver.

global deformation of a piece of rubber mounted as shown in Figure 4c. During each interaction, the tool tip moved in straight line in the direction of the normal to the undeformed sample surface.

Figure 5a gives an example of tool displacement trajectory. Figures 5b and 5c, collect overlaid force-deflection curves resulting from the contact with these tools. The force-deflection curves for three different tools are almost identical. The small difference between the loading and the unloading phase of each test is due to a small amount of energy loss. It can easily be explained either by a slight sliding movement of the tool over the body surface or by plastic deformation of the body.

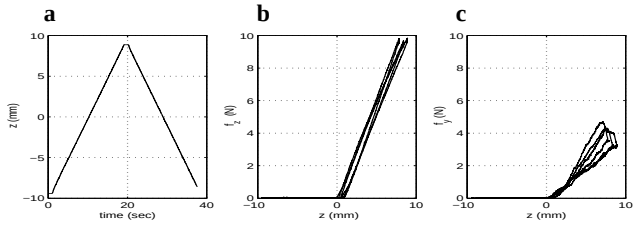

Figure 5: A Deflection trajectory and force-deflection curves for contact of three tool shapes.

4.2 Case of Localized Deformation

In the second test, the effect of tool shape on normal contacts with local deformation was studied. The rubber sample was mounted so as to be held by a large traction surface as shown by Figure 4d. Figure 6a, gives an example of tool displacement trajectory and Figure 6b collects overlaid force-deflection curves. The curves of the tools are now significantly different from each other. We compare the force-deflection curves of each tool with the analytical solution for a normal contact of the same tool with an infinite half space (the value $E^* = 3.45$ MPA was identified). For forces smaller than $12N$, the analytical solutions fit the measurements almost exactly.

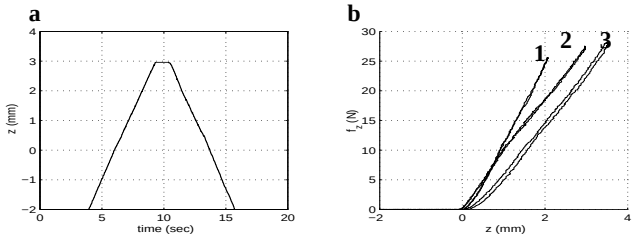

Figure 6: Displacement trajectory and force deflection curves for tool shapes: **1)** 12.7 mm sphere, **2)** flat, and **3)** 3.2 mm sphere.

4.3 Extensible Deformable Body

In the third experiment, we investigated whether the tool shape had a significant effect on the force-deflection responses of tool contact with an extensible deformable body. The body was a rectangular prism of fresh calf liver 10 mm deep, see Figure 4e. Figure 7a provides an example of tool displacement trajectory and Figure 7b, collects overlaid force-deflection curves resulting from contacts of the spherical tools. The flat tool was not tested since it tended to damage the sample. Force-deflection responses of the tools were significantly different.

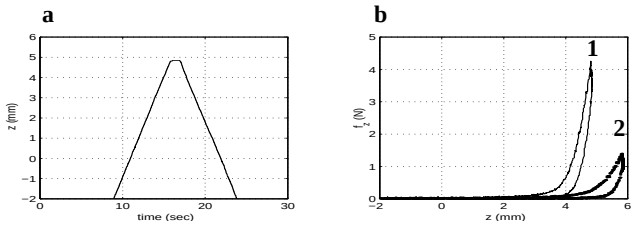

Figure 7: Displacement and force for tools: **1)** 12.7 mm sphere and **2)** 3.2 mm acting on the liver sample.

4.4 Normal Force Invariance

In the fourth experiment, the effect of the normal force of a sliding contact was investigated with a 3.2 mm spherical tool and the rubber sample, see Figure 4d. The normal

contact was along z and the sliding movement along x axis. In the first phase, the normal force was brought to around 14 N, and then several sliding back and forth displacements were performed over the flat surface of the rubber. This created a wide range of friction forces, from -7 N to 7 N.

Figures 8a and 8b show the displacement trajectories and figures 8c and 8d show the force trajectories. Figures 8e and 8f show plots of the corresponding force-displacement curves. As Figure 8c,e shows, during sliding movements, the amplitude of normal force did not change significantly.

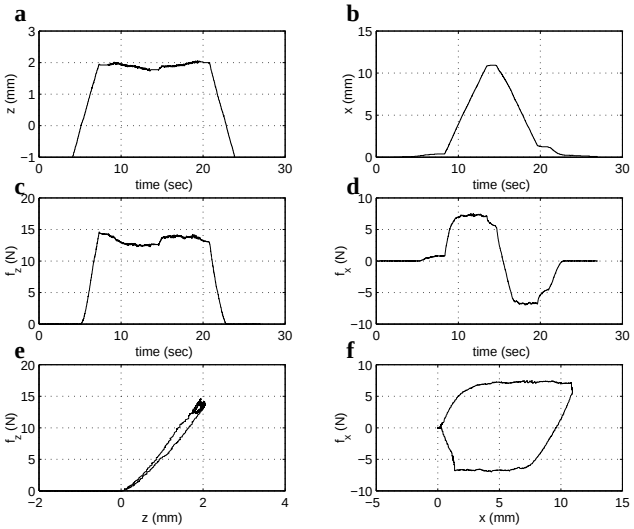

Figure 8: Displacements and forces during normal and sliding contact between a spherical tool and the flat surface of a rubbery piece.

5 Implementation

The model was implemented to evaluate its performance. It also allowed us to empirically assess the effect of tool shape on the haptic experience.

The forces were rendered by a PenCat/Pro^{TM} haptic device (Immersion Canada Inc.). The simulation program consisted of two independent real-time threads running under RTlinux3. One thread provided for rendering of the forces. A separate user process provided for graphics and user interaction with Tcl/Tk. The graphical user interface can be seen in Figure 9.

The virtual body was intently chosen to be a large cylinder. This allowed us to use the analytical solutions of contact mechanics. The surface of the cylinder was meshed into triangular elements. At each vertex the normal vector is along the radius of the cylinder so the force deflection response along that normal is the analytical solution corresponding to a material and a tool shape selected by the user. The tool shapes could be flat cylindrical punches, cones, and spheres of different radius [10]. The force-deflection equations can be seen at Table 1.

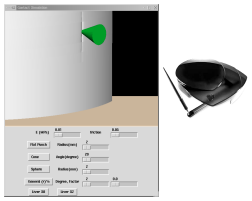

Figure 9: Graphical user interface and device used in the tool contact simulation.

Due to the high update rate, the rendering was completely free of oscillations and limit cycles. The analytical force solution guaranteed continuity resulting in a very realistic experience. The arbitrary selection of tool shapes and material properties allowed to confirm as these factors affect significantly the haptic experience.

6 Conclusion

This paper studied cases of interaction between a tool and a deformable body where the force displacement response is needed for haptic rendering purposes. It was found that when the energy supplied by the tool distributes everywhere in the body, corresponding to the case when the deflections of the contact neighborhood are not significantly different, the force-displacement response does not depend on the tool shape or on the form of contact. This is not true however when the body undergoes significant localized deformation. The tool force-displacement response in this case critically depends on tool shape and the form of contact.

A model for computing tool force-displacement responses of interactions with localized deformation was introduced. The response to a normal contact with a tool could easily be calculated at run time by interpolation of pre-calculated force-deflection responses. A computer implementation of the model was described that allowed to assess the effect of tool geometry in contact rendering.

Our approach essentially bypasses the constraint of real-time computation of contact response using preprocessing. The storage requirements are quite modest. This approach can be generalized to cases that include other tool maneuvers, global deformation, and even cutting [12]. The workspace of the interaction is discretised into small workspaces over which contact responses are chosen to be piecewise interpolated between pre-calculated contact samples. Depending on the application, various approximations can be made in an informed fashion to trade accuracy with storage and complexity.

For the graphic simulation of contact interaction with local deformation, we used the analytical solutions of contact mechanics. However the methods of computation of deformation in computer graphics [6, 8] could be used to represents the visual appearance. Graphics and haptics should be done as separate processes as the constraints, models and hardware are completely different. However graphics and haptic process could share some aspects of the simulation such as the determination of the contact position. Also, graphics process could benefit from the knowledge of accurate contact solutions provided by haptics process.

7 Acknowledgements

This research is funded by the project "Reality-based Modeling and Simulation of Physical Systems in Virtual Environments" supported by IRIS-III, the Institute for Robotics and Intelligent Systems which is part of Canada's Network of Centers of Excellence program (NCE). Additional funding is provided by NSERC, the Natural Sciences and Engineering Council of Canada, in the form of an operating grant for the second author.

References

[1] Astley, O., Hayward, V. 1998. Multi-rate Haptic Simulation Achieved by Coupling Finite Element Meshes Through Norton Equivalents. *Proc. IEEE Int. Conf. on Robotics and Automation*, pp. 989-994.

[2] Aulignac, D. , Balaniuk, R., Laugier, C. April 2000. A Haptic Interface for a Virtual Exam of the Human Thigh, *ICRA2000*, San Francisco, USA.

[3] Bro-Nielsen, M. 1998. Finite Element Modeling in Surgery Simulation. *Proceedings of the IEEE*, 86:3, pp. 490–503.

[4] Debunne, G., Desbrun, M., Cani, M., Barr, A. 2001. Dynamic Real-Time Deformations Using Space and Time Adaptive Sampling. *Computer Graphics*, Siggraph 2001, Los Angeles.

[5] Cotin, S., Delingette, H., Ayache, N. 1999. Real-time Elastic Deformations of Soft Tissues for Surgery Simulation. *IEEE Transactions on Visualization and Computer Graphics*, 5:1, pp. 62–73.

[6] Gibson, S. F. F., Mirtich, B. 1997. A Survey of Deformable Modeling in Computer Graphics. *Tech. Rep. TR97-19*, Mitsubishi Electronic research Laboratories, Cambridge, MA.

[7] Hayward, V., Armstrong, B. 2000. A New Computational Model of Friction Applied to Haptic Rendering. In *Experimental Robotics VI*, P. I. Corke and J. Trevelyan (Eds.), Lecture Notes in Control and Information Sciences, Vol. 250, Springer-Verlag, pp. 403-412.

[8] James D. L. and Pai D. K. 1999. ArtDefo, Accurate Real time Deformable Objects. *SIGGRAPH 99 Conference Proceedings*. pp. 65-72.

[9] James, D. L., Pai D. K. 2001. A Unified Treatment of Elastostatic and Rigid Contact Simulation for Real Time Haptics. *Haptics-e, the Electronic Journal of Haptics Research*. Vol. 2, No. 1.

[10] Johnson, K. L. 1987. *Contact Mechanics*. Cambridge University Press.

[11] Langhaar, H. L. 1962. *Energy Methods in Applied Mechanics*. John Wiley and Sons, Inc.

[12] Mahvash, M., Hayward, V. 2000. Haptic Rendering of Cutting, A Fracture Mechanics Approach. *Haptics-e, the Electronic Journal of Haptics Research*. Vol. 2, No. 3.

[13] Pai D. K., Lang J., Lloyd J. E., Woodham, R. J. 2000. ACME, a Telerobotic Active Measurement Facility. In *Experimental Robotics VI*, P. I. Corke and J. Trevelyan (Eds.), Vol. 250 of Lecture Notes in Control and Information Sciences, pp. 391–400, Springer-Verlag.

[14] Rao, S. S. 1999. *The Finite Element Method in Engineering Third Edition*, Butterworth-heinemann, 3 edition.

[15] Ruspini, D. C., Kolarov K., Khatib, O. 1997. Haptic Interaction in Virtual Environments. Proc. *IROS*.

[16] Wu, X., Downes, M. S. , Goktekin, T., Tendick, F., 2001. Adaptive Nonlinear Finite Elements for Deformable Body Simulation Using Dynamic Progressive Meshes. Proc. *Eurographics 2001*, vol. 20, no. 3, pp. 349-58.

[17] Zilles, C. B., Salisbury. J. K. 1995, A Constraint-based God Object Method for Haptic Display. Proc. *IEEE Int. Conf. Intel. Rob. and Syst.*, Vol. 3, pp. 146–151.

[18] Zhuang, Y., Canny, J. 2000. Haptic Interaction with Global Deformations. Proc. *IEEE Robotics and Automation Conference*, IEEE, Vol.3, pp. 2428–2433.